I&EC research
Industrial & Engineering Chemistry Research

pubs.acs.org/IECR

Article

Technoeconomic Evaluation of the Industrial Implementation of Catalytic Direct Nonoxidative Methane Coupling

Rolf S. Postma, Dylan J. Keijsper, Bart F. Morsink, Erwin H. Siegers, Muhammed E. E. Mercimek, Lance K. Nieukoop, Henk van den Berg, Aloijsius G. J. van der Ham, and Leon Lefferts*

Cite This: https://doi.org/10.1021/acs.iecr.1c03572

Read Online

ACCESS | Metrics & More | Article Recommendations | Supporting Information

ABSTRACT: This paper presents a process design for catalytic nonoxidative natural gas conversion to olefins and aromatics, highlighting the opportunities and challenges concerning industrial implementation. The optimal reactor conditions are 5 bar and 1000 °C. Heat exchange over the reactor is challenging due to the high temperature and low gas pressure. Recovery of ethylene is economically unattractive due to the low ethylene concentration in the product stream, leading to a methane-to-aromatics process, recycling ethylene. Benzene is the most valuable product at an efficiency of 0.31 $kg_{benzene}/kg_{methane}$ with hydrogen as a major valuable byproduct. Naphthalene, with a low value, is unfortunately the dominant product, at 0.52 $kg_{naphthalene}/kg_{methane}$. It is suggested to hydrocrack the naphthalene to more valuable BTX products in an additional downstream process. The process is calculated to result in a 107 $ profit per ton CH_4.

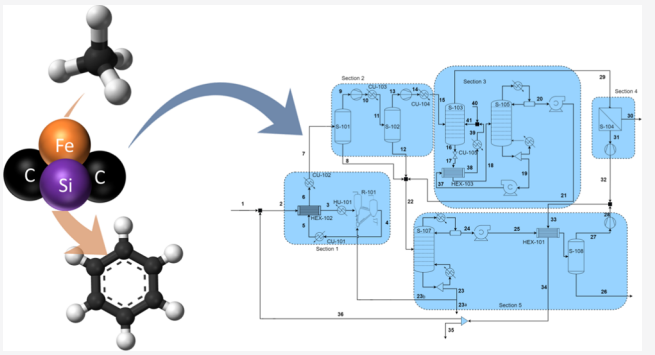

1. INTRODUCTION

Natural gas is seen as a high-potential intermediate source of base chemicals, such as ethylene and benzene,[1−5] replacing crude oil in the change toward renewable sources for energy and chemicals. Currently, the production of bulk chemicals, such as ethylene and benzene, is based on petroleum feedstock.[6,7] The well-known natural gas reserve is around 2 × 10^{15} m^3.[6,76,7] The global usage is expected to increase from 4.1 × 10^{12} $m^3{\cdot}y^{-1}$ in 2020[8] to 5.75 × 10^{12} $m^3{\cdot}y^{-1}$ in 2040, an average growth of 3.0% a year.[9] This can be attributed to the increased production of natural gas with a high methane content as seen in the exploitation of shale gas and tight oil.[10] A result of this increased production is an expected significant drop in the future price of natural gas compared to crude oil. Both residential and commercial heating, as well as the production of power are a major part of the total natural gas consumption. The use of natural gas and other fossil fuels to generate energy is not sustainable due to the high greenhouse gas emissions and the resulting impact on the climate. Furthermore, renewable energy sources such as wind and solar are expected to take over the energy and heating requirements for both residential and industrial applications.[11−16] Due to the decreasing natural gas price and slow phase-out of natural gas as an energy carrier, it remains economically interesting to evaluate the possibilities to use natural gas as a feedstock for chemical synthesis.

1.1. Industrial State of the Art. There are already several industrial processes for converting methane into hydrocarbons, most of which are based on multiple conversion steps, starting with syngas production.[17−19] Syngas is produced by steam reforming of natural gas over nickel catalysts.[20] Common synthesis routes starting from syngas include Fischer−Tropsch (FT) synthesis to paraffinic waxes, methanol synthesis, and ammonia synthesis.[17−19,21−24] An FT-based process generally uses Fe- or Co-based catalysts to convert syngas into linear aliphatic hydrocarbons. The catalyst as well as process conditions dictate the chain growth and thus the product distribution. Generally, FT synthesis is followed by cracking the products to lower alkanes and olefins,[25] yielding an overall carbon efficiency between 60 and 65%.[26] Methanol can be converted into gasoline using the methanol-to-gasoline (MTG) process, in which methanol is first dehydrated over an acid catalyst to dimethyl ether, which is subsequently converted into a gasoline blend.[27] The full route from natural gas to higher hydrocarbons using either the FT or MTG reactions is called the "gas-to-liquid" (GTL) process. To date, the largest industrial plant using the FT technology is the Shell Pearl GTL plant converting 4.5 × 10^7 $m^3{\cdot}day^{-1}$ natural gas to hydrocarbons.[28] Along the same line, the methanol-to-olefin

Received: September 3, 2021
Revised: November 18, 2021
Accepted: November 24, 2021

(MTO) process shows great promise as a source of olefins from methane.[22,23] MTO starts with steam reforming methane to syngas, followed by methanol synthesis. The methanol is converted to light olefins, such as ethylene and propylene. The advantages of MTO over GTL are the production of more valuable products and a more narrow product distribution.[17,23] MTO has already been commercialized on a smaller scale by DICP and UOP,[29,30] while other companies already developed process designs.[30,31]

The disadvantages of any indirect route for methane coupling to higher hydrocarbons are the inevitable production of oxygen-containing byproducts (water and CO_2) as well as the required separation and purification between each consecutive synthesis step.[32] All current industrial methane conversion processes require large installed capacities to become economically viable,[33] making them unattractive for smaller remote gas fields. Pipelines and cryogenic transport for centralized methane conversion are generally too costly to be viable.[3,34,35] For this reason, many small gas fields, for instance, at the coast of Australia remain unexploited.[36] Also, many relatively small and remote (shale-) oil fields in the United States resort to flaring or venting to get rid of their co-produced natural gas, leading to unnecessary greenhouse emissions.[37] Direct coupling of methane to higher hydrocarbons is likely economically more attractive for operation at small capacity[3] compared to alternatives, due to the reduced number of process steps and limited variation under process conditions. This would make direct methane coupling interesting as an on-site process for smaller oil and gas fields, especially if the product is liquid under ambient conditions. The different methods for converting methane to different higher hydrocarbons, both industrially applied and academically investigated, are summarized in Figure 1.

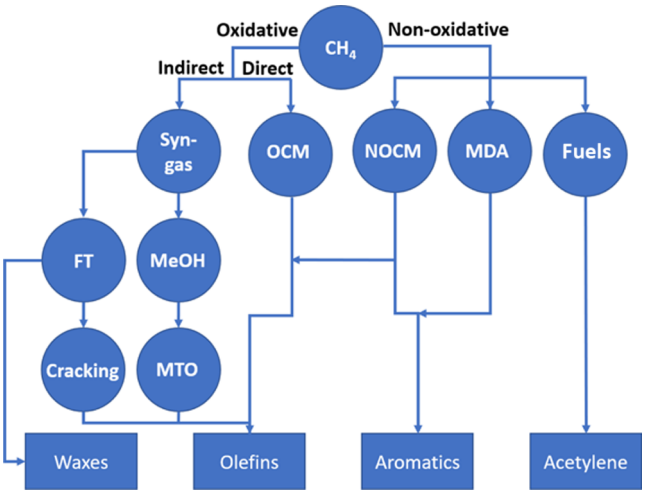

Figure 1. Different conversion strategies for methane into higher hydrocarbons; the explanation of the abbreviations can be found at the end of this paper.

Direct coupling of methane has seen a steady increase in research over the last years for these reasons. This research is focused on three potential strategies:

1. methane dehydroaromatization (MDA)[4,19,38−40]
2. oxidative coupling of methane (OCM)[19,41]
3. nonoxidative coupling of methane (NOCM)[32,42−51]

1.2. Methane Dehydroaromatization. MDA is a process in which methane is directly converted to lower aromatics, such as benzene and naphthalene.[4] Generally, the catalysts used consist of a transition metal (e.g., Mo) supported on a zeolite (e.g., ZSM-5). Confinement in the pores of the zeolite is responsible for the selectivity toward aromatics rather than coke. Galadima et al.[4] reviewed results obtained with several metal-modified zeolites in the MDA reaction. The general drawbacks of the MDA reaction are low product yields, low single-pass methane conversion, and high coking rates. The highest single-pass aromatic yield of 11% is obtained at 700 °C and atmospheric pressure with a 6 wt % Mo/H-ZSM-5 catalyst, as reported by Zhao et al.[52] The single-pass methane conversion is low due to the unfavorable equilibrium at a reaction temperature of around 700 °C.[4] Figure 2 shows that at

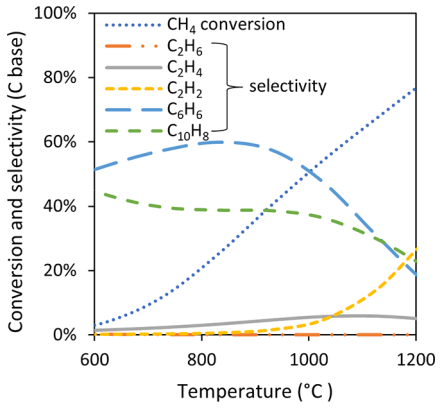

Figure 2. Thermodynamic equilibrium methane conversion and carbon-based product selectivity based on the thermodynamic data presented by Guéret et al.[53]

700 °C, the maximum theoretical methane conversion is 11% when coking is not taken into account. In general, MDA suffers from high coking rates, requiring catalyst regeneration within a time span of minutes.[4]

1.3. Oxidative Coupling of Methane. Oxidative coupling of methane (OCM) circumvents the thermodynamic restrain shown in Figure 2, by dosing small amounts of oxidant (oxygen or sulfur) in the reactant mixture. The thermodynamic equilibrium shifts to a higher methane conversion via oxidation of the hydrogen product. The main product group of OCM is light olefins, with CO_2 and water as significant byproducts. OCM was first reported in 1982,[54] sparking a worldwide research surge.[55,56] Hundreds of catalytic materials have since been synthesized and tested, mostly in the 1990s and also in recent years.[5] Ideally, the oxidant is only used to decrease the methane activation barrier, after which the formed methyl radicals react to C_2 hydrocarbons.[57] Unfortunately, the presence of O_2 leads to significant oxidation of the formed hydrocarbons, limiting the single-pass hydrocarbon yield to below 30%, at 60% C_{2+} selectivity.[3,5] Thus, the carbon utilization efficiency of OCM remains relatively low.[58,59] Process modeling showed that OCM can only be economically viable if single-pass conversions and C_2 selectivity are at least 30% and 90% respectively.[60,61] Therefore, even the Bi-Y-SM catalyst reporting the highest C_2 yield thus far[62] at 28% conversion and 53% selectivity does not approach the industrial requirements

1.4. Nonoxidative Coupling of Methane. Catalytic nonoxidative coupling of methane (NOCM) is generally used

https://doi.org/10.1021/acs.iecr.1c03572
Ind. Eng. Chem. Res. XXXX, XXX, XXX−XXX

Table 1. General Overview of Specifics Obtained from Process Designs for the Three Types of Catalytic Reactions to Convert Methane to Higher Hydrocarbons

CH_4 conv. method	MDA	OCM	NOCM
C_2 single-pass yield	1%[64]	30 C%[3,5]	9 C%[32]
aromatic single-pass yield	11%[4]	N/A	39 C%[32]
coke selectivity	28%[4]	N/A	0%,[32,42] 12%[43,51]
	32% (1 bar), 12% (10 bar)[64]		
economic viability requirements	conversion > 25%	conversion > 30%	conversion > 32%
	HC selectivity > 30%[65]	C_2 selectivity > 90%[60,61]	HC selectivity > 80%[22]
byproducts	H_2 & coke	H_2O & CO_2	H_2 & coke
carbon efficiency	31%[65]	60%[3,5]	100%[22,32]
			83%[66]

as an overarching term for nonoxidative routes to methane coupling. We have opted to exclude MDA from this category because MDA requires an additional steric effect to steer selectivity, which warrants its own section. NOCM generally operates at even a higher temperature, above 900 °C, to achieve industrially relevant methane conversion (i.e., >10% conversion),[53] as illustrated in Figure 2. Hydrogen is co-produced as a valuable byproduct, while the formation of coke can pose practical limitations such as catalyst deactivation, process disorder, as well as carbon yield loss. In 2014, Guo et al.[32] reported a Fe/SiO_2 catalyst, capable of converting CH_4 nonoxidatively to ethylene, benzene, and naphthalene. Crucially, it was claimed that this catalyst does not cause coke formation, even at a high conversion level, i.e., 48% at 1080 °C. A constant molar ethylene selectivity of ∼50% was reported for temperatures between 950 and 1080 °C. Atomically dispersed Fe(II) sites on silica are postulated to selectively dehydrogenate CH_4 to methyl ($CH_3^{\bullet}$) radicals, initiating free-radical coupling reactions in the gas phase. This has been supported with DFT calculations by Kim et al.[50] Guo et al.[32] named this specific catalyst Fe©SiO_2, and this notation will also be adopted in this paper. Sakbodin et al.[42] demonstrated that methane conversion over the Fe©SiO_2 catalyst can be significantly boosted by introducing a hydrogen-permeable membrane in the reactor to remove hydrogen in situ. Oh et al.[43] demonstrated that a coated wall reactor using Fe©SiO_2 also causes an increase in methane conversion. Han et al.[44] reported that SiO_2 in the cristobalite crystal phase is required to minimize coke formation, requiring the high fusion temperature during catalyst preparation (1700 °C). Furthermore, the atomic dispersion of Fe prevents coke formation on the active site of the catalyst. Our previous work[51] showed experimentally that the catalyst is only required for methane activation, after which propagation occurs in the postcatalytic volume, which can also be deducted from the examples presented in a recent patent by SABIC.[63] Other types of catalysts have also been reported for the NOCM reaction,[45−49] but these show low conversion, high coking rates, or are only tested at low CH_4 partial pressures.

1.5. Process Designs Concerning Direct Coupling of Methane. The reported high conversion and high resistance to coking of Fe©SiO_2 are interesting for possible industrial application. However, the severe reaction conditions, as well as the broad product distribution, present various challenges in terms of process design. Many process design studies concerning the single-step conversion of methane focused on MDA and OCM reactions.[61,65,67−72] In contrast, there are currently only two papers on process design addressing high-temperature catalytic NOCM.[22,66] The general conclusions from these process designs studies are summarized in Table 1. The product yields and coke selectivity in Table 1 are the best experimental results reported in the literature. The economic viability requirement shows the minimum single-pass methane conversion and hydrocarbon selectivity required.

Huang et al.[22] performed a study to screen how certain conditions affect the net present value (NPV) of an NOCM process. A detailed process design including economic evaluation is presented, and the process design is evaluated starting from a base case, in which process and economic variables are systematically varied, to evaluate the sensitivity for the NPV. The base case evaluated assumes the following conditions and productivity $T_{conversion}$: 800 °C, CH_4 single-pass conversion: 25%, coke selectivity: 0% and ethylene selectivity: 20 C%, the benzene and naphthalene selectivities are both 30 C% with the remaining 20 C% divided over minor olefins and aliphatics (i.e., ethane, propane, propylene, butane, and butene). This base case is actually not realistic when looking at Figure 2, which shows that the maximum methane conversion based on thermodynamics, without allowing coking, is 20% at 800 °C. They concluded that the single-pass conversion of methane and coke selectivity are the main parameters affecting profitability. The single-pass conversion of methane should be above 25% and coke selectivity should not exceed 20%. Furthermore, they concluded that profitability can be increased by increasing olefin yield over aromatic yield, as expected. Do et al.[66] performed a technoeconomic feasibility study of a direct methane coupling process, similar to Huang et al.[22] After the conversion step, all products are systematically removed, starting with the aromatics and ending with cryogenic recovery of the produced ethylene. The reactor is operated at 1200 °C and atmospheric pressure, and it is stated that product distribution is assumed, without further details. They conclude that the most important factors determining profitability are the cost of natural gas and electricity as well as the sales price of ethylene. Unfortunately, the importance of minimum conversion and selectivity was not discussed.

Several points have not been addressed so far when evaluating the industrial application of NOCM in addition to the selection of the reaction conditions:

1. Separation scheme of the products, byproducts, and unconverted reactant.
2. Heat supply to the reactor, considering the endothermicity of the reaction (see Table 2), as well as the intensive heat transfer required between feed and product streams.
3. Strategy for operating the reactor, considering coking.
4. Regeneration of the catalyst/reactor in the case of coking

https://doi.org/10.1021/acs.iecr.1c03572
Ind. Eng. Chem. Res. XXXX, XXX, XXX−XXX

Table 2. Standard (1 atm, 25 °C) Enthalpy Change of the Three Considered Reactions, Normalized Per Carbon Atom

reaction	STD enthalpy change (kJ·mol$_C^{-1}$)[73]	STD Gibbs energy change (kJ·mol$_C^{-1}$)[74]
$2CH_4 \rightleftharpoons C_2H_4 + 2H_2$	101.1	−16.6
$6CH_4 \rightleftharpoons C_6H_6 + 9H_2$	88.1	−29.9
$10CH_4 \rightleftharpoons C_{10}H_8 + 16H_2$	89.2	−37.9

This paper presents a detailed design of a plant using the Fe©SiO_2 catalyst to convert natural gas using the NOCM reaction. The main aim is to evaluate possible solutions for the above four challenges, using proven industrial technologies. The insights obtained will give directions for both further research on the catalyst and on other technologies required. Note that many of the aspects discussed in this paper are general to any NOCM reaction and not specific to the Fe©SiO_2 catalyst.

2. PROCESS DESIGN

The scope of the design is a process with a capacity of 200 ktpa benzene with a purity of 99.8 wt % based on the Fe©SiO_2 catalyst to convert natural gas using the NOCM reaction. Catalyst performance data, concerning both activity and selectivity, have been taken from the original work on the Fe©SiO_2 catalyst by Guo et al.[32] It must however be noted that other papers[42−44,50,51,63] reporting on this catalyst showed a broader product range of minor products, including ethane, acetylene, C_{3-5} olefins, and alkylbenzenes. The selectivity to these products becomes negligible at a higher methane conversion[75] and is therefore not included to reduce complexity. In this study, a standard composition for dry natural gas in the United States is used, presented in Table 3.[76,77] It is assumed that all hydrocarbons are alkanes.

Table 3. Composition of Natural Gas Found in the US Gulf Coast Area[76,77]

component	mole fraction (%)	trace components	amount
N_2	1.25	S-components	5.5 mg·m^{-3}
CH_4	91.01	H_2O	<65 mg·m^{-3}
C_2	4.88	O_2	0.01 mole %
C_3	1.69	CO_2	0.01 mole %
C_4	0.66		
C_5	0.27		
C_6	0.13		
C_7 and above	0.11		

2.1. Methodology. The applied design methodology is based on the method described by Douglas and is derived from the book "Conceptual Design of Chemical Processes".[78] The selection of the separation method is based on the selection schemes published by Barnicki and Fair.[79,80]

Various alternatives were identified, and the least attractive were rejected based on heuristics, as recommended by Douglas.[78] Several iterations were made, ending up with the final operation block diagram as presented in Figure 3. The final flowsheet was evaluated using Aspen Plus.[81] Note that exclusively the heat exchanger over the reactor has been included in Figure 3, due to its importance for both the process design (further explained in Section 2.8) and process economics (explained in Section 2.9).

2.2. Gas Pretreatment. Natural gas contains many impurities as shown in Table 3. It is likely that these impurities will poison or foul process steps and need to be removed. All sulfur-containing compounds are removed using a caustic scrubber, which also removes any CO_2. It is chosen to leave all hydrocarbons in the feed stream, to maximize carbon utilization and to prevent high separation costs for removing the C_{2+} hydrocarbons at these concentrations. It is assumed that the natural gas has already been cleaned before entering the process.

2.3. Physical and Chemical Consideration for the Reaction. All studies concerning the NOCM reaction reported thus far were performed at atmospheric or subatmospheric pressures.[32,42−49] This is highly undesirable from a design perspective because low pressures require larger volumes for the installed reactor and additional unit operations such as heat exchangers. Furthermore, low pressures are highly disadvantageous for gas−gas heat exchange. In addition, higher pressures are required to facilitate the separation of the products. This clearly shows the requirement for the reactor to operate at elevated pressures. Kosinov et al.[64] reported that increasing pressure from 1 to 15 bar reduces coke selectivity from 33 to 11% and also increased catalyst productivity from 33 to 160 mmolCH_4·g_{cat}^{-1} in the MDA reaction.

$$xCH_4 \rightleftharpoons C_xH_y + \left(2x - \frac{y}{2}\right)H_2 \quad (1)$$

The NOCM reaction results in a considerable increase in volume, due to the significant co-production of hydrogen (eq 1). Le Chatelier's principle dictates that at a higher pressure, the equilibrium of eq 1 will favor the reactant side and thus methane conversion will be limited. The equilibrium methane conversion as a function of total pressure was modeled, using Aspen Plus,[81] allowing ethylene, benzene, naphthalene, and hydrogen as products (Figure 4). The reported minimum single-pass conversion for a feasible methane coupling process is between 25 and 30% depending on the process.[22,60,61] The influence of pressure on the maximum achievable conversion in the reactor was estimated by correcting the conversion achieved by Guo et al.[32] at 1 atm and 1000 °C along the

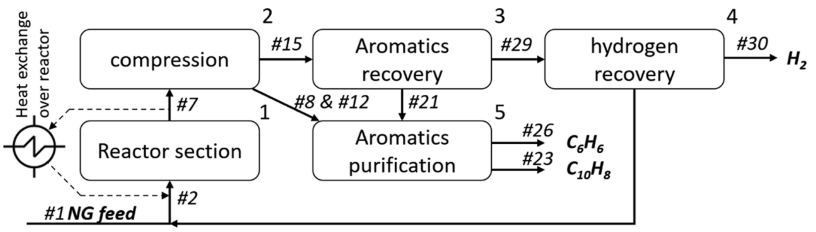

Figure 3. Functional block diagram of the designed process for direct coupling of methane using the Fe©SiO_2 catalyst; for more details, see Figure 5 and Table 5.

https://doi.org/10.1021/acs.iecr.1c03572
Ind. Eng. Chem. Res. XXXX, XXX, XXX−XXX

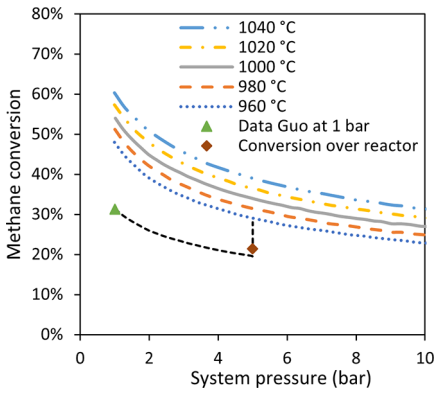

Figure 4. Methane conversion at thermodynamic equilibrium as a function of reactor pressure at temperatures ranging from 960 to 1040 °C, calculated using Aspen Plus,[81] using a Gibbs reactor allowing for the formation of ethylene, benzene, naphthalene, and hydrogen; The color-coded triangles represent the maximum reported experimental conversion at 1000 °C[32] (all at 1 bar).

equilibrium line shown in Figure 4. It was found that 5 bar is the optimal pressure for the reactor operated at 1000 °C, resulting in a 19.7% single-pass methane conversion. Kosinov[64] reported decreasing coke formation on increasing pressure; assuming a similar effect in our case results in a methane conversion of 28% at 5 bar. C_{2-4} hydrocarbons as well as the hydrogen and inert entering the reactor are passed through an equilibrium converter to calculate the lowest Gibbs free energy. The equilibrium converted produces a significant amount of methane, resulting in an overall methane conversion of 21.4% over the reactor. Details concerning these calculations are found in Sections S.1.1 and S.1.2 in the Supporting Information.

The selectivity data presented by Guo et al.[32] at 1000 °C and 1 atm pressure will be used because this is the only paper that reports data measured at industrially relevant conversion levels. The selectivity values have been corrected for the increase in pressure, as described in detail in SI Section 1.2. The selectivity values are presented in Table 4. Note that the reported selectivity distribution is already close to thermodynamic equilibrium compared to Figure 2, the main difference is a higher ethylene selectivity.

Table 4. Assumed Carbon Selectivity of Methane toward the Three Carbon-Containing Products Based on Ref32

hydrocarbon product	carbon selectivity
ethylene (C_2H_4)	21 C%
benzene (C_6H_6)	26 C%
naphthalene ($C_{10}H_8$)	53 C%

The reactor feed contains not only methane but also small amounts of C_{2+} hydrocarbons (percentage level), as shown in Table 3. These hydrocarbons are significantly less stable under reaction conditions compared to CH_4. Guo et al.[32] showed that the addition of small amounts of ethane to the reaction mixture will both cause a significant increase in reaction rate and co-produce coke. Ethane and ethylene are potent free-radical initiators,[75,82−85] significantly enhancing methane conversion. It can be safely assumed, based on experimental data,[75] that increasing the space velocity can largely prevent coke formation due to C_{2+} hydrocarbons while keeping the same conversion as a consequence of increasing reaction rate. However, it is unlikely that coke formation can be completely prevented by tuning the space velocity. Unfortunately, there is no information on the effect of addition of small amounts of C_{3+} hydrocarbon on the performance of the NOCM reaction. Therefore, it is assumed in the model that coking from C_{2-4} hydrocarbons can be prevented but that all C_{5+} hydrocarbons will react swiftly to coke. In reality, all C_{2+} hydrocarbons will cause the formation of some deposits. Note that a variance in the coke selectivity will not significantly impact the carbon balance of the process, as long as fuel combustion is required to overcome the endothermicity of the reaction. More details concerning the impact of the assumed coking rate will be given in Section 2.5.

2.4. Process Overview. A detailed overview of the process can be seen in Figure 5. Cleaned makeup-gas enters stream #1 and is mixed with the recycle stream #36. It passes through a heat exchanger (HEX-102) and a furnace (HU-101) before entering the reactor (R-101). An FCC-type reactor has been chosen for continuous coke removal from the catalyst, more details concerning the reactor are given in Section 2.5. The product gas from the reactor is first quenched to 600 °C in an oil quencher (CU-101) to stabilize the product mixture after the reactor and prevent further coupling and coke formation and fouling of equipment. The stream after the quench (#5) is further cooled with the feed stream (#2) in a heat exchanger (HEX-102). In R-101, the NOCM reactions proceed at 5 bar and 1000 °C as discussed in the previous section. In section 2, the product gas is compressed first from 5 to 35 bar, using compressors with interstage coolers CU-103 and CU-104 and condensate separators (S-101 and S-102) to remove any aromatic condensates. After compression, the remaining aromatic species are removed (in section 3) in an absorption column using sulfolane (S-103). After regeneration of the sulfolane (S-105), the aromatic streams from the condensate separators (streams 8 and 12) as well as the absorption section (stream 21) are mixed and upgraded in section 5 by distillation (S-107) to get the products benzene (#24) and naphthalene (#23). Part of the naphthalene stream (#23b) can be split off to use in both furnace HU-101 and the reactor (R-101) to cover the heating duty, with the remainder of the naphthalene in stream #23a. The benzene stream is cooled and treated in a phase separator (S-108) to reach the final purity of 99.8%. The aromatic-free product stream (#29) of the absorber S-103 continues to the membrane section (section 4) for hydrogen separation (S-104). The remaining hydrocarbon stream (#32), consisting mainly of methane and low concentrations of ethylene, is mixed with stream #28 from the benzene purification section and recycled to the reactor inlet and mixed with the fresh feed stream. The recycle contains a purge (#35) of 2% to prevent the buildup of inert impurities in the system. The stream size and composition concerning these sections are presented in Table 5. The choices made in the sequence and techniques used for product separation and purification are detailed in the section below.

2.5. Reactor Design. The reactor performance (i.e., conversion and selectivity) has been estimated and fixed in this process design because of the uncertainties in performance of nonoxidative coupling of methane reaction with respect to the effects of operating conditions on methane conversion, selectivity distribution, and coking rates, as discussed in Section 2.3. Reactor design consideration will still be discussed below, due to the high importance of reactor design on process performance.

https://doi.org/10.1021/acs.iecr.1c03572
Ind. Eng. Chem. Res. XXXX, XXX, XXX−XXX

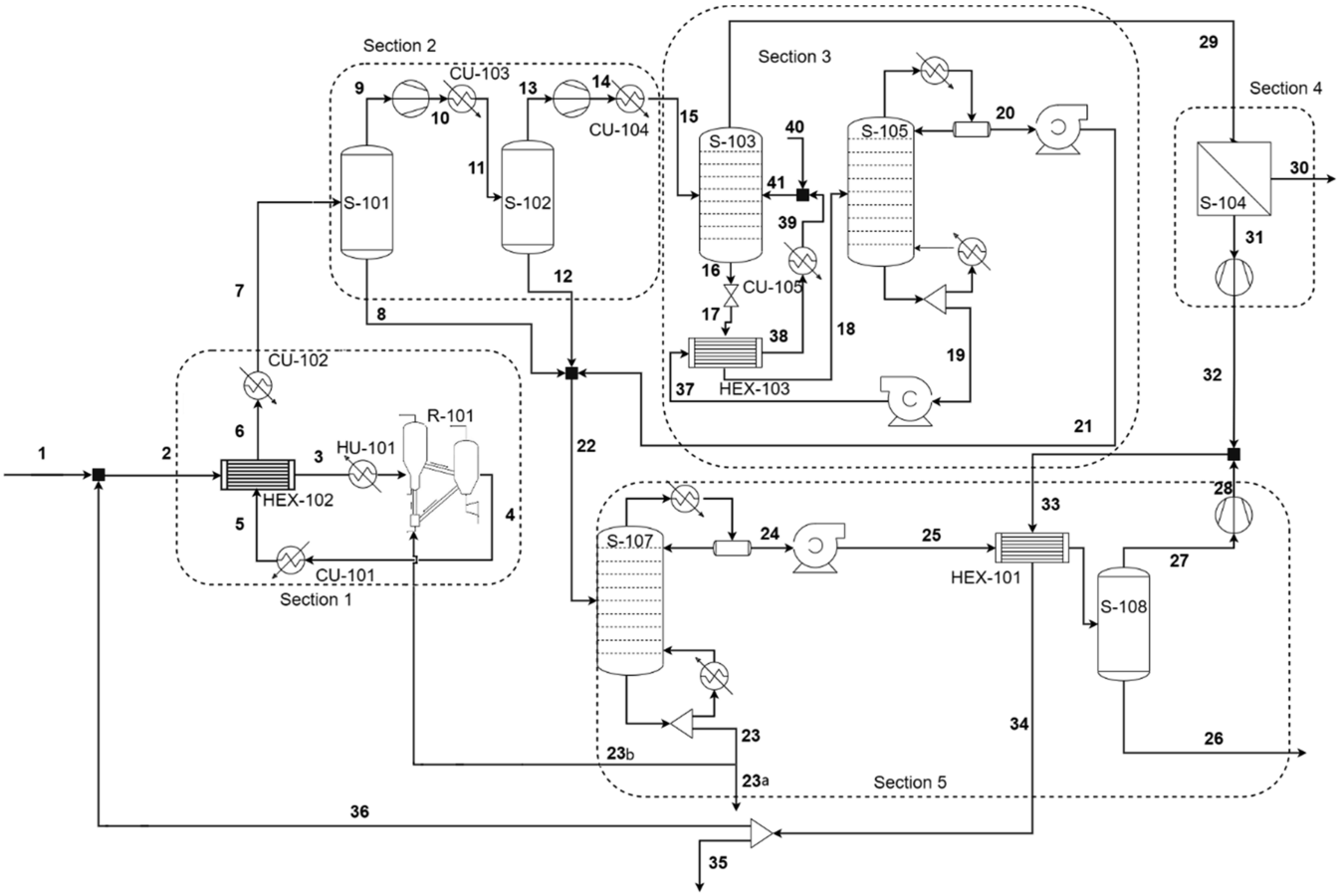

Figure 5. Process flow diagram, divided into five operational sections, based on function. Section 1 is the conversion section, concerning the reactor and heating and cooling. Section 2 concerns the compression of the product stream, with intermediate flash tanks to remove any condensing aromatics. Section 3 removes the remaining aromatics from the product stream. Section 4 consists of membranes to separate most of the hydrogen. Section 5 concerns the aromatic purification.

Preheating in the heat exchanger HEX-102 in section 1, Figure 5, is limited to 600 °C to prevent coke formation in the feed before reaching the catalyst bed. Heating from 600 to 1000 °C in HU-101 must be realized as quickly as possible in the reactor, just upstream of the catalyst bed.[51] The required heat input for preheating the feed from 600 to 1000 °C is calculated at 165 MW (2.0 MJ/$kg_{methane}$). The reaction itself is highly endothermic, as shown in Table 2. The required heat amounts to 142 MW (1.7 MJ/$kg_{methane}$), calculated with Aspen Plus,[81] resulting in a total heat input for the furnace HU-101 and the reactor R-101 of 307 MW (3.7 MJ/$kg_{methane}$) (Table 6). This sizable heat input can be accommodated in various ways: first, 61 MW can be accommodated by burning the purge gas (mainly methane, stream #35) and another 10 MW can be obtained by burning the formed coke during catalyst regeneration. The remaining 236 MW can be generated by (i) burning part of the naphthalene, from stream #23; (ii) burning the hydrogen, from #30, produced in the process; (iii) by burning part of the methane process feed; or (iv) by electric heating. Burning hydrogen and electric heating, at 4 $ct·$kWh^{-1}$,[86] are both deemed too expensive in the current market, although both options will significantly reduce the CO_2 emissions of the process. Natural gas is the cheapest option for supplying the required heat.[87,88] However, for this process design, it was chosen to use the naphthalene as a heat source for the remaining 236 MW, due to the large quantity of naphthalene produced as well as the limited market size.[89]

Using the lower heating value of 38.9 MJ·kg^{-1},[88] it can be calculated that 6.0 kg·s^{-1} naphthalene is required, out of 10 kg·s^{-1} from stream #23 (Figure 5 and Table 5). Providing the required heat to the reactor section will be very challenging, due to the high required heating rate to prevent coking.[51] The feed can be heated from 600 to 1000 °C with a multitubular gas-fired heater (unit HU-101 in Figure 5), comparable to a cracking furnace. It is imperative to make the thermal driving force as large as possible, as well as supplying an inert lining on the inside of the tubes, to prevent heterogeneous activation of methane and especially higher hydrocarbons. The method to add heat for the endothermicity of the reaction depends on the choice of reactor. In a fluidized bed reactor, such as an FCC-type reactor, the heat can be supplied by preheating the catalyst. The catalyst is synthesized at 1700 °C[32] and is therefore expected to be stable up to ∼1600 °C. As discussed above, 10 MW of heat can be produced by burning the coke on the catalyst during regeneration. The rest of the reaction heat (142 - 10 = 132 MW) is supplied by burning the naphthalene. Assuming the catalyst is cooled from 1600 to 1000 °C during the reaction, this would result in a catalyst recirculation rate of 310 kg·s^{-1} (resulting in a catalyst-to-gas mass flow ratio of 3:1). This catalyst recirculation rate can be lowered, or even a fixed-bed operation can be used, if the heat is supplied through additional multitubular gas-fired heaters, similar to preheating of the gas.

https://doi.org/10.1021/acs.iecr.1c03572
Ind. Eng. Chem. Res. XXXX, XXX, XXX−XXX

Table 5. Conditions and Molar Flows of the Main Streams Represented in Figure 5[a]

stream	1	2	7	8	12	15	21	22	23	26	28	29	30	31	34	35
T (°C)	20	21	90	90	90	90	210	152	250	20	105	94	94	94	21	21
P (bar)	5	5	5	5	12	35	2	2	2	2	5	35	1	35	5	5
n (Mmol·h^{-1})	4.7	22	24	0.23	0.05	23	0.42	0.69	0.28	0.28	0.13	23	7.1	16	16	0.32
CH_4 (mol %)	91.0	83.0	55.6	0.39	0.98	56.2	24.2	14.8	0	0.45	78.3	56.8	4.1	80.6	80.5	80.5
C_2H_6 (mol %)	4.9	1.1	0.01	0	0	0.01	0.01	0.01	0	0	0.04	0.01	0	0.01	0.01	0.01
C_2H_4 (mol %)	0	2.2	2.0	0.05	0.13	2.0	3.0	1.9	0	0.29	9.3	2.0	0.08	2.9	2.9	2.9
C_6H_6 (mol %)	0	0.09	1.3	4.7	11.4	1.3	64.8	41.6	0	99.2	5.0	0.05	0	0.08	0.12	0.12
$C_{10}H_8$ (mol %)	0	0.01	1.2	94.6	87.4	0.11	5.6	40.3	99.8	0.01	0	0.01	0	0.01	0.01	0.01
H_2 (mol %)	0	4.1	32.4	0.01	0.03	32.8	0.7	0.45	0	0	2.4	33.4	95.5	5.4	5.4	5.4
N_2 (mol %)	1.3	8.8	7.5	0.02	0.06	7.6	1.6	0.95	0	0.01	5.0	7.7	0.34	11.1	11.0	11.0
other (mol %)	2.9	0.68	0	0.25	0.02	0	0	0	0.19	0.01	0.01	0	0	0	0.01	0.01

[a]The content and conditions of all other flows are presented in Supporting Information S.2; note that most streams omitted from this table have got the same composition as the ones presented, for example, streams 4, 5, and 6 have the same composition as stream 7, but different temperatures. The composition of stream 36 is also equal in composition to 34 and 35, Mmol refers to megamole, i.e., 10^6 mole.

Table 6. Parameters Chosen or Calculated for the Reactor; Selectivities Are Shown in Table 4

reactor parameter	chosen or calculated value
temperature	1000 °C
pressure	5 bar
single-pass methane conversion	28%
single-pass C_2+ conversion	100%
required heat input: preheating feed	165 MW
required heat input: reaction endothermicity	142 MW
total required heat input to reactor	307 MW

Coking will likely occur in the reactor, independent of the catalyst or reactor design, as discussed above. This coke has to be removed from the reactor to prevent deactivation, fouling, or blocking. Two types of industrial reactors will be able to handle these conditions, namely, an FCC type of reactor,[90] with an independent conversion and regeneration section, or a Catofin reactor,[91] where conversion and regeneration are handled in a simulated moving-bed arrangement. The FCC reactor is optimal for high coking rates, leading to deactivation in a time span from seconds to minutes, whereas a Catofin reactor is most useful when regeneration is required between tens of minutes to hours. The FCC reactor was chosen for this process design, as coking rates are probably significant, leading to the formation of a monolayer of coke on the catalyst in 36−80 s. This assumption is based on the time required for the C_5 components to form a monolayer of graphitic carbon on the surface of the catalyst.[91] Furthermore, our previous work[51] showed that limiting the contact time in the catalyst bed, in favor of longer gas-phase residence time at a high temperature, increases productivity while decreasing deposit formation. The increase in total hydrocarbon yield when minimizing catalyst residence time was also demonstrated in a recent SABIC patent.[63] It must be noted that the results published by Guo et al.,[32] used as performance data for the FCC reactor in this process design, were measured on the lab scale in a fixed-bed reactor. As discussed in the process overview, an oil quencher will be used to quickly bring down the temperature and stabilize the product mixture after the reactor, as proposed and shown in an example in a recent SABIC patent.[63]

2.6. Separation Parameters. It is best practice to evaluate first the separation of the largest product fraction, as described by Douglas et al.[78] and Barnicki and Fair.[79,80] In this case, the main product from the NOCM reaction is hydrogen, accounting for up to 32 vol % of the reactor outlet stream, as can be seen in Table 5. All hydrogen separation technologies considered tend to foul in the presence of aromatic compounds,[92−94] and naphthalene will condense at the used temperature and pressure ranges. Thus, deep aromatic removal is required as the first separation step. Deep aromatic removal is most easily achieved with an absorption process using sulfolane as a solvent, commonly used in the industry for aromatic separation.[7] It was also considered to use the produced naphthalene, or high-boiling oil as a solvent, but this did not yield the required separation efficiency. Other options considered and evaluated were a simple flash or a distillation column. Both either did not yield the required separation or were too costly due to the required temperatures.

The sulfolane is recovered by means of distillation. The resulting aromatic streams are combined and distilled to obtain pure benzene stream (#26, 99.2 %) and pure naphthalene stream (#23, 99.8%)

https://doi.org/10.1021/acs.iecr.1c03572
Ind. Eng. Chem. Res. XXXX, XXX, XXX−XXX

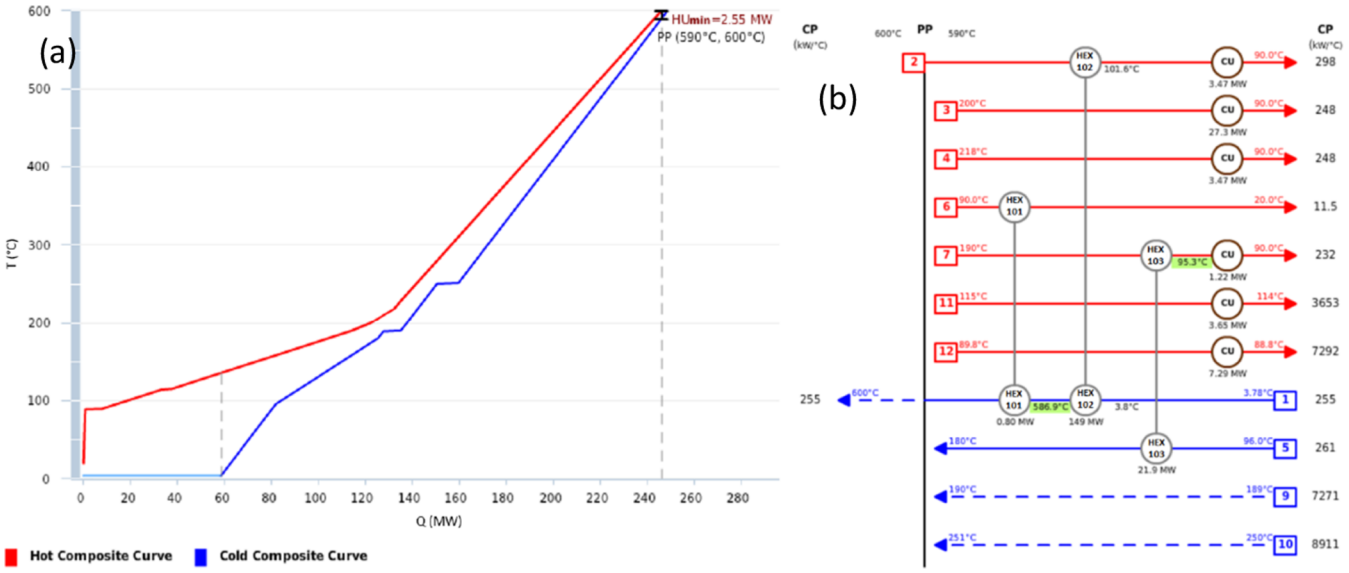

Figure 6. (a) Composite curve following the pinch study; (b) heat exchanger network developed based on the pinch study.

Polymeric membranes are the most suitable option for hydrogen separation,[92−95] based on their maturity in the industry as well as the process conditions. This results in a hydrogen stream with 95.5 vol % purity, which can be further increased by the use of PSA, although this is out of the scope of this study. Other evaluated options include different types of membranes, i.e., palladium, silica, or carbon-based membrane,[88,96−100] and direct pressure swing adsorption (PSA).[101] The concentration of hydrogen in stream #29 is lower than required for PSA separation,[101] although this technique can be used to further purify the permeate stream (#30) and thus increase the value of the produced hydrogen. Palladium membranes are too expensive,[96] silica membranes tend to suffer from rapid degradation and have not yet seen industrial use,[100] and carbon-based membranes have thus far not been used for separating hydrogen from hydrocarbon mixtures.

The remaining stream after hydrogen separation contains mainly methane with percentage amounts of ethylene, around 3 vol % at this stage; see Table 5, stream #31. Cryogenic distillation is the only ethylene recovery method applied at a large scale.[102] The separation costs per ton of ethylene is estimated at 1900 $\$\cdot ton^{-1}$(see Supporting Information S.3), significantly more than the 2020 ethylene retail price of 1000 $\$\cdot ton^{-1}$.[103] A more energy-efficient method to separate ethylene from methane is needed, or the ethylene concentration should be at least doubled, to make the recovery viable. For this reason, all ethylene is recycled back into the reactor, converting it further to benzene and other aromatics. This results in the loss of 104 $kton\cdot y^{-1}$ ethylene, for a total gross value of 104 $mln\$\cdot y^{-1}$ in ethylene, although it must be noted that the ethylene is converted into benzene, naphthalene, and hydrogen in the recycle, thus minimizing the value lost.

2.7. Carbon Efficiency. The total carbon efficiency of the process amounts to 86%, based on the mass balance in Table 5. This value becomes 54 % when discounting for the naphthalene burned for supplying the heat to the reactor. These values are in the ballpark of the current Fischer−Tropsch style processes, which operate at carbon efficiencies between 60 and 65%.[26] Unfortunately, the process yield of benzene is only 32% based on carbon, and the rest of the carbon ends up in naphthalene. Therefore, naphthalene upgrading to added-value products is necessary. Currently, naphthalene is used as a precursor to phthalic anhydride, as well as various azo-dyes and pesticides.[104] Naphthalene can be selectively hydrocracked to mono-aromatic hydrocarbons, using a blend of hydrogen and methane as cracking agents, at 400 °C and 40 bar.[105] Full naphthalene conversion was achieved after 1 h in an autoclave, using Zn/HY as a catalyst. The main products are toluene and propane.

Hydrogen is also a major product of the NOCM process, which should be considered a valuable product in the emerging hydrogen economy.[106]

2.8. Heat Integration and Pinch Study. The total heating duty required in the process without heat integration is 187 MW and the total cooling duty amounts to 247 MW (9.8 and 13.0 $MJ/kg_{methane}$ fed to the process, respectively). This includes the heating of the reactor feed to 600 °C. However, it excludes the preheating of the reactor feed from 600 to 1000 °C, the endothermic heat input for the reactor, as well as the cooling duty required in the initial quenching of the product mixture from 1000 to 600 °C after the conversion reactor. These heat duties are left out since they cannot be used for heat integration due to the high required heating and cooling rates to prevent coke formation,[51] as explained in the reactor design section. The heat in the oil used for the direct quench of the reactant mixture is exchanged to generate high-pressure steam. Direct oil quenching was selected to reduce the risk of fouling. An alternative is the use of indirect quenching using a heat exchanger, which generates the high-pressure steam directly.[6]

The heat integration evaluation for this process is based on a pinch study using 10 °C as the temperature difference at the pinch. The resulting composite curves can be found in Figure 6a. The pinch temperature is at 600 °C, which means that all streams evaluated are below the pinch and only cooling utility is needed. Based on the composite curve, a network of heat exchangers and coolers is developed, presented in Figure 6b and also incorporated in the PFD (Figure 5). The first heat exchanger (HEX-101 in Figure 5) is used to cool the benzene stream from distillation column S-107 before it is flashed to remove any remaining lighter hydrocarbons (S-108), and the

https://doi.org/10.1021/acs.iecr.1c03572
Ind. Eng. Chem. Res. XXXX, XXX, XXX−XXX

cooling is done with the expanded gases of the recycle. The second heat exchanger (HEX-102 in Figure 5) is used to heat the reactor feed and cool the product stream. Note that this heat exchanger needs to exchange 149 MW of heat (1.4 MJ/Kg_{stream}), which considering the heat exchange between two gas streams results in 68 000 m^2 of heat-exchange area required, due to the low ΔT of 10°C at the pinch. The third heat exchanger (HEX-103) is used to heat the feed of the sulfolane recovery distillation column (S-105) while cooling the returning lean sulfolane from the reboiler of the distillation column, after which only a cooling duty of about 45 MW is left, which will be handled by cooling water since it is below 140 °C.

Considering the very large required surface area for heat exchange and similarly large investment costs associated with HEX-102, it needs to be reevaluated. An increase in minimum temperature difference over the heat exchanger will significantly reduce the required surface area for heat exchange, at the cost of requiring additional heating and cooling duty. If both the costs of HEX-102 and the additional costs of extra required cooling and heating are taken into account, calculated over the depreciation period of 10 years, assuming 15% interest per year over the investment, one obtains Figure 7. It is clear

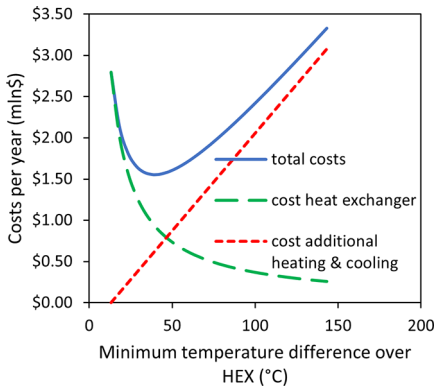

Figure 7. Optimization costs of the main heat exchanger (HEX-102), considering a depreciation period of 10 years.

that the costs for both installing HEX-102 combined with the additional heating and cooling will be minimal at a minimum temperature difference of 40 °C, which is a reasonable value for gas−gas heat exchangers. The size of the heat exchanger can be reduced to 20 000 m^2 heat exchange area at this temperature difference but does require both 8 MW additional heating and cooling. Although 20 000 m^2 is still a very large heat exchanger, it is technically feasible. Note that the additional costs for heating and cooling equipment are not taken into account for this calculation. These optimization calculations are not included in the final economic evaluation, due to the low impact.

2.9. Economic Evaluation. The plant economics are calculated in US$ in the year 2018, for a benzene production capacity of 200 ktpa. Equipment was sized using basic design principles. The capital expenditure (CAPEX) for the equipment was estimated using a combination of cost estimation tools.[107−109] Equipment costs are estimated using the tools from Matche[107] and Equipment Costs correlations published in Plant Design and Economics for Chemical Engineers.[108] The scaling factors for inside and offside battery limits (ISBL and OSBL) described by Sinnot et al.[109] are used to adjust for installation costs, piping, and other auxiliaries, generally resulting in a Lang factor of 6 (Table 7). The CAPEX cost

Table 7. Purchased Cost of the Main Process Equipment, the Applied Lang Factor, and the Corresponding Total Capital Investment (TCI)

equipment	purchased cost (mln $)	Lang factor	TCI (mln $)
HEX	32.3	6	194
pump	0.02	6	0.1
compressors	25.4	6	152
columns	1.2	6	7.3
reactor	120.7	1	121
mixers	0.2	6	1.1
membranes	6.1	1	6.1
total (ISBL)			481
total (ISBL + OSBL)	(OSBL = 40% of ISBL)		700

was corrected for inflation to 2018 using the Chemical Engineering Plant Cost Index (CEPCI). Note that the used costs for the reactor as well as the membrane section already include installation costs; thus, their Lang factor was kept at 1. Table 7 shows the capital expenditure split over the different types of installed units, note that "columns" includes both the distillation equipment and the flash drums. Using the ISBL and OSBL factors, the total capital expenditure is also shown in Table 7. Note that the inaccuracy of CAPEX costs can be up to 30%, especially considering the uncertainty surrounding the optimal reactor design.

Table 8 presents the costs of raw material, product revenue, and utility costs. The amounts are based on the mass and energy balance from Table 5. Note that Table 8 shows the results for two situations: (1) 60% of the naphthalene is used for heating the reactor and the rest is sold; (2) naphthalene is completely sold (results given within parentheses), while natural gas will be used for heating the reactor feed (corresponding value within parentheses). These options will both result in significant CO_2 emissions, making the process not environmentally friendly. Technologies like carbon capture and storage (CCS) can be used to mitigate this effect but will result in a significant increase in cost. Other heating options considered include hydrogen as a fuel or electric heating, but these are both expensive and will yield a large naphthalene product stream without a sizable market. This can only be solved by another process that converts naphthalene (for instance, by hydrocracking) into marketable products. It is assumed that catalyst losses are negligible, due to the long-term stability.[32] The hydrogen price is relatively low as a result of the low purity achieved by the membrane. The designed process does not produce any organic waste streams requiring treatment, as all waste streams containing hydrocarbons are combusted for heat generation. The spent catalyst will be returned to the manufacturer.

Table 9 presents the auxiliary costs of the process, namely, the costs of wages, technical assistance, and overhead. We have chosen to also include the depreciation of the capital expenditure in this table, assuming total depreciation of the plant over 10 years.

Table 10 calculates the total profitability of the process, taking into account the information from Tables 7−9. Furthermore, the sales, R&D, administration, and management costs are included as well as profit tax.

https://doi.org/10.1021/acs.iecr.1c03572
Ind. Eng. Chem. Res. XXXX, XXX, XXX−XXX

Table 8. Overview of Total Raw Material Costs, Product Revenue, and Utility Costs for Two Situations[a][110]

raw material costs			
components	price ($·ton^{-1})	amount (kton·year^{-1})	total cost (mln$·year^{-1})
natural gas	125[87]	739 (897)	92 (112)
sulfolane	3000[111]	0.6	2
catalyst	3000 (own estimation)	1	3
total (mln$·year^{-1})	97 (117)		
product revenue			
components	**price ($·ton^{-1})**	**amount (kton·year^{-1})**	**revenue (mln$·year^{-1})**
benzene	860[112]	194	167
naphthalene	450[113]	123 (314)	55 (142)
hydrogen	800[114]	119.5	95.6
steam (from CU-101)	12.1[109]	2890	35
total (mln$·year^{-1})	353 (440)		
utility costs			
components	**price**	**amount (year^{-1})**	**total costs (mln$·year^{-1})**
electricity	40$/MWh[109]	399 GWh	16
cooling water	13 × 10^{-3}$/m^3[109]	52.4 × 10^6 m^3	0.7
steam	12.1 $/ton[109]	126 kton	1.5
total (mln$·year^{-1})	18.1		

[a]Values outside parentheses indicate that naphthalene is partly combusted for reactor heating. Values within parentheses indicate that naphthalene is fully sold and extra natural gas is combusted for heating the reactor. The estimates for the costs and replenishment rate of the catalyst are based on the FCC process.[110]

Table 9. Auxiliary Operational Costs, Including Wages, Services, Property Tax and Insurance, and Depreciation of the CAPEX, as Presented in Table 7

fixed costs	remarks	OPEX cost (mln$·year^{-1})
operating labor including supervision	5 shifts of 10 operators each	5.0
overhead		2.5
maintenance		30.0
property tax and insurance	1% of TCI	7.0
depreciation	10% of TCI	70.0
total		114.0

Table 10. General Expenses, Taxes, and Total Profitability of the Process, Taking into Account the Figures Shown in Tables 8 and 9

general expenses (GE)	% of revenue	total (mln$)
sales	3.0%	10.5
R&D	5.3%	18.5
administration	2.0%	7.0
management	4.0%	14.0
total		50.0
OPEX + GE	279.0	
profit before tax		74
tax	20% of profit	15
total profit		59

The total profitability for the base case process is calculated to be 59 mln$·y^{-1} after taxes. It is clear that a methane coupling process can potentially be very profitable, provided natural gas is relatively cheap and abundantly available. Even though this process design is as much as possible based on proven industrial techniques and processes, it is still based on various significant assumptions in terms of conversion, product selectivity, and costs. Figure 8 presents a sensitivity analysis from the base case presented in Tables 7 and 8. The sensitivity analysis presented in Figure 8a shows that the product price (especially the price of benzene) mainly determines the profitability of the process. This shows that the profitability can increase considerably if the marketability of naphthalene increases. Figure 8b shows that the natural gas price also has a significant impact on profitability. The range of 50% is appropriate for natural gas, whose price fluctuated by an average of 30% on annual basis between 2000 and 2020 in the US market, decreasing by 50% over this total period.[115] The market price of benzene fluctuates significantly less at an average of 13% per year, although 2020 saw a drop of 51% in benzene price.[116] These values were not available for naphthalene and hydrogen, although it can be safely assumed that the hydrogen price will closely follow the natural gas price. Figure 8c also shows that the CAPEX determines the profitability only to a limited extent, which is positive considering the high CAPEX estimated for the reactor and main heat exchanger (HEX-102) and its uncertainty.

3. CONCLUSIONS

The technoeconomic evaluation of a detailed process design for catalytic direct conversion of methane to olefins and aromatics shows a significant economic potential of 107 $ profit per ton CH_4 fed, to convert relative cheap natural gas into valuable benzene (0.31 $kg_{benzene}/kg_{methane}$) and hydrogen. Naphthalene (0.52 $kg_{naphthalene}/kg_{methane}$) is a significant byproduct, which is mainly combusted in the current process design for heating the reactor with the consequent emission of CO_2. If electrical heating or hydrogen combustion is used, a large quantity of naphthalene will be available, saturating the current market. It is therefore necessary to look for other processes to convert naphthalene into valuable products, such as monoaromatics. The profitability of the process is mainly determined by the product prices with a dominant role for benzene and hydrogen.

The process also has several challenges such as integrated heating of the gaseous feed (with the gaseous product) and the heating of the reactor itself with duties of 165 MW (2.0 MJ/$kg_{methane}$) and 142 MW (1.7 MJ/$kg_{methane}$), respectively. The excessive heat exchanger area can be reduced by operating at a higher temperature difference and 40 °C is estimated to be optimal, increasing the heating and cooling duty. The suggested reactor for this process is an FCC-type reactor operated at a pressure of minimum 5 bar, using the catalyst as the heat transfer medium at the same time. Both the primary heat exchanger and the reactor account for almost 2/3 of the total investment costs, due to their required capacity and extreme condition (1000 °C). Any optimization regarding these units can result in a significant decrease in process costs.

Several critical assumptions are on the basis of the design that needs to be validated, for instance, the conversion and selectivity at 5 bar and 1000 °C, effect of carbon deposition on catalyst activity, and the effect of higher concentrations of

https://doi.org/10.1021/acs.iecr.1c03572
Ind. Eng. Chem. Res. XXXX, XXX, XXX−XXX

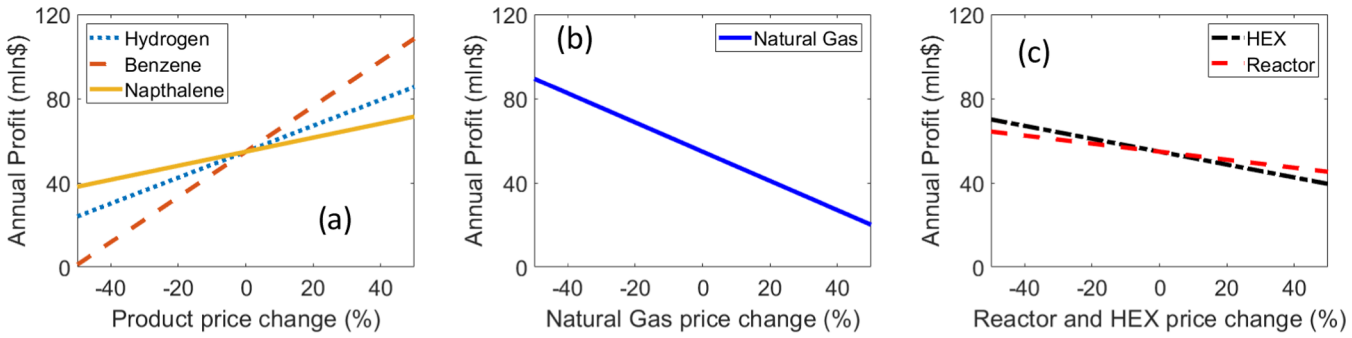

Figure 8. Sensitivity of key process factors on the profitability of the catalytic NOCM process: (a) product prices, (b) natural gas costs, and (c) the main investment cost of the reactor and the main heat exchanger.

hydrocarbons (C_{2+}) in the reactor feed on both reactivity and carbon deposit selectivity.

The minimum required reactor pressure is 5 bar. It is suggested to test reaction performance at increased pressure, as well as effects concerning impurities in the feed, i.e., C_{2-5} hydrocarbons. Current industrial hydrogen separation techniques are sensitive to fouling and require low temperatures. Therefore, deep aromatics removal is required before hydrogen purification. Finally, the heat exchangers needed at the reactor are large and require significant additional heating and cooling, due to the large duty in combination with the low heat transfer coefficient. Overall, an increase in pressure in the reactor will lead to a lower heat-exchange area and less compression required for the separation. Experiments should validate if adequate natural gas conversion can be reached at elevated pressure.

■ ASSOCIATED CONTENT

Supporting Information

The Supporting Information is available free of charge at https://pubs.acs.org/doi/10.1021/acs.iecr.1c03572.

Methane conversion and product selectivity calculations, information on all streams depicted in Figure 5, and calculations concerning the economics of ethylene recovery (PDF)

■ AUTHOR INFORMATION

Corresponding Author

Leon Lefferts − *Catalytic Processes and Materials Group, Faculty of Science and Technology, MESA+ Institute for Nanotechnology, University of Twente, Enschede 7500 AE, Netherlands;* orcid.org/0000-0003-2377-5282; Email: l.lefferts@utwente.nl

Authors

Rolf S. Postma − *Catalytic Processes and Materials Group, Faculty of Science and Technology, MESA+ Institute for Nanotechnology, University of Twente, Enschede 7500 AE, Netherlands;* orcid.org/0000-0001-7150-4407

Dylan J. Keijsper − *Sustainable Process Technology, Faculty of Science and Technology, University of Twente, Enschede 7500 AE, Netherlands*

Bart F. Morsink − *Sustainable Process Technology, Faculty of Science and Technology, University of Twente, Enschede 7500 AE, Netherlands*

Erwin H. Siegers − *Sustainable Process Technology, Faculty of Science and Technology, University of Twente, Enschede 7500 AE, Netherlands*

Muhammed E. E. Mercimek − *Sustainable Process Technology, Faculty of Science and Technology, University of Twente, Enschede 7500 AE, Netherlands*

Lance K. Nieukoop − *Sustainable Process Technology, Faculty of Science and Technology, University of Twente, Enschede 7500 AE, Netherlands*

Henk van den Berg − *Sustainable Process Technology, Faculty of Science and Technology, University of Twente, Enschede 7500 AE, Netherlands*

Aloijsius G. J. van der Ham − *Sustainable Process Technology, Faculty of Science and Technology, University of Twente, Enschede 7500 AE, Netherlands*

Complete contact information is available at: https://pubs.acs.org/10.1021/acs.iecr.1c03572

Notes

The authors declare no competing financial interest.

■ ACKNOWLEDGMENTS

The authors acknowledge support from the Dutch National Science Foundation (NWO) and the industrial partners SABIC, Sasol, and BASF.

■ ABBREVIATIONS USED

FT	Fischer−Tropsch
MTO	methanol to olefins
GTL	gas to liquids
MDA	methane dehydroaromatization
OCM	oxidative coupling of methane
NOCM	nonoxidative coupling of methane
NPV	net present value
Ktpa	kilo ton per annum (year)

■ REFERENCES

(1) Mesters, C. A Selection of Recent Advances in C1 Chemistry. *Annu. Rev. Chem. Biomol. Eng.* **2016**, *7*, 223−238.

(2) Karakaya, C.; Kee, R. J. Progress in the direct catalytic conversion of methane to fuels and chemicals. *Prog. Energy Combust. Sci.* **2016**, *55*, 60−97.

(3) Taifan, W.; Baltrusaitis, J. CH4 conversion to value added products: Potential, limitations and extensions of a single step heterogeneous catalysis. *Appl. Catal., B* **2016**, *198*, 525−547.

(4) Galadima, A.; Muraza, O. Advances in Catalyst Design for the Conversion of Methane to Aromatics: A Critical Review. *Catal. Surv. Asia* **2019**, *23*, 149−170.

(5) Gao, Y.; Neal, L. M.; Ding, D.; Wu, W.; Baroi, C.; Gaffney, A.; Li, F. Recent Advances in Intensified Ethylene Production − A Review. *ACS Catal.* **2019**, *9*, 8592−5621.

https://doi.org/10.1021/acs.iecr.1c03572
Ind. Eng. Chem. Res. XXXX, XXX, XXX−XXX

(6) Zimmermann, H.; Walzl, R. Ethylene. In *Ullmann's Encyclopedia of Industrial Chemistry*; Wiley-VCH Verlag GmbH & Co. KGaA, 2009.
(7) Folkins, H. O. Benzene. In *Ullmann's Encyclopedia of Industrial Chemistry*; Wiley-VCH Verlag GmbH & Co. KGaA, 2000.
(8) *Gas 2020*; IEA: Paris, 2020.
(9) Conti, J.; Holtberg, P.; Diefenderfer, J.; LaRose, A.; Turnure, J. T.; Westfall, L. *International Energy Outlook 2016*; U.S. Energy Information Administration, 2016.
(10) McFarland, E. Unconventional Chemistry for Unconventional Natural Gas. *Science* **2012**, *338*, 340−342.
(11) Abbasi, H.; Benson, C.; Briselden, T.; Angelini, P.; Brooks, D. *Roadmap for Process Heating Technology*; Industrial Heating Equipment Association, 2001.
(12) Orella, M. J.; Román-Leshkov, Y.; Brushett, F. R. Emerging opportunities for electrochemical processing to enable sustainable chemical manufacturing. *Curr. Opin. Chem. Eng.* **2018**, *20*, 159−167.
(13) Yeh, S.; Lutsey, N. P.; Parker, N. C. Assessment of Technologies to Meet a Low Carbon Fuel Standard. *Environ. Sci. Technol.* **2009**, *43*, 6907−6914.
(14) Wismann, S. T.; Engbæk, J. S.; Vendelbo, S. B.; Bendixen, F. B.; Eriksen, W. L.; Aasberg-Petersen, K.; Frandsen, C.; Chorkendorff, I.; Mortensen, P. M. Electrified methane reforming: A compact approach to greener industrial hydrogen production. *Science* **2019**, *364*, 756−759.
(15) Karytsas, S.; Theodoropoulou, H. Public awareness and willingness to adopt ground source heat pumps for domestic heating and cooling. *Renewable Sustainable Energy Rev.* **2014**, *34*, 49−57.
(16) Valancius, R.; Singh, R. M.; Jurelionis, A.; Vaiciunas, J. A Review of Heat Pump Systems and Applications in Cold Climates: Evidence from Lithuania. *Energies* **2019**, *12*, No. 4331.
(17) de Klerk, A. Fischer−Tropsch Process. In *Kirk-Othmer Encyclopedia of Chemical Technology*, 2013; pp 1−20.
(18) Wittcoff, H. A.; Reuben, B. G.; Plotkin, J. S. *Chemicals from Methane*; John Wiley & Sons, Inc, 2012.
(19) Kee, R. J.; Karakaya, C.; Zhu, H. Process intensification in the catalytic conversion of natural gas to fuels and chemicals. *Proc. Combust. Inst.* **2017**, *36*, 51−76.
(20) Abdulrasheed, A.; Jalil, A. A.; Gambo, Y.; Ibrahim, M.; Hambali, H. U.; Hamid, M. Y. S. A review on catalyst development for dry reforming of methane to syngas: Recent advances. *Renewable Sustainable Energy Rev.* **2019**, *108*, 175−193.
(21) Wang, B.; Albarracín-Suazo, S.; Pagán-Torres, Y.; Nikolla, E. Advances in methane conversion processes. *Catal. Today* **2017**, *285*, 147−158.
(22) Huang, K.; Miller, J. B.; Huber, G. W.; Dumesic, J. A.; Maravelias, C. T. A General Framework for the Evaluation of Direct Nonoxidative Methane Conversion Strategies. *Joule* **2018**, *2*, 349−365.
(23) Amghizar, I.; Vandewalle, L. A.; Geem, K. M. V.; Marin, G. B. New Trends in Olefin Production. *Engineering* **2017**, *3*, 171−178.
(24) Appl, M. Ammonia. In *Ullmann's Encyclopedia of Industrial Chemistry*, 2011.
(25) Wood, D. A.; Nwaoha, C.; Towler, B. F. Gas-to-liquids (GTL): A review of an industry offering several routes for monetizing natural gas. *J. Nat. Gas Sci. Eng.* **2012**, *9*, 196−208.
(26) Panahi, M.; Yasaria, E.; Rafiee, A. Multi-objective optimization of a gas-to-liquids (GTL) process with staged Fischer-Tropsch reactor. *Energy Convers. Manage.* **2018**, *163*, 239−249.
(27) ExxonMobil Chemicals MTG Factsheet; 2018.
(28) PEARL GTL. https://www.shell.com.qa/en_qa/about-us/projects-and-sites/pearl-gtl.html (accessed 14-05-2020).
(29) Tian, P.; Wei, Y.; Ye, M.; Liu, Z. Methanol to Olefins (MTO): From Fundamentals to Commercialization. *ACS Catal.* **2015**, *5*, 1922−1938.
(30) Chen, J. Q.; Bozzano, A.; Glover, B.; Fuglerud, T.; Kvisle, S. Recent advancements in ethylene and propylene production using the UOP/Hydro MTO process. *Catal. Today* **2005**, *106*, 103−107.
(31) Ren, T.; Patel, M. K.; Blok, K. Steam cracking and methane to olefins: Energy use, CO2 emissions and production costs. *Energy* **2008**, *33*, 817−833.
(32) Guo, X.; Fang, G.; Li, G.; Ma, H.; Fan, H.; Yu, L.; Ma, C.; Wu, X.; Deng, D.; Wei, M.; Tan, D.; Si, R.; Zhang, S.; Li, J.; Sun, L.; Tang, Z.; Pan, X.; Bao, X. Direct, Nonoxidative Conversion of Methane to Ethylene, Aromatics, and Hydrogen. *Science* **2014**, *344*, 616−619.
(33) Mohajerani, S.; Kumar, A.; Oni, A. O. A techno-economic assessment of gas-to-liquid and coal-to-liquid plants through the development of scale factors. *Energy* **2018**, *150*, 681−693.
(34) Rui, Z.; Metz, P. A.; Reynolds, D. B.; Chen, G.; Zhou, X. Historical pipeline construction cost analysis. *Int. J. Oil, Gas and Coal Technology* **2011**, *4*, No. 244.
(35) Jin, C.; Lim, Y. Optimization and economic evaluation of integrated natural gas liquids (NGL) and liquefied natural gas (LNG) processing for lean feed gas. *Appl. Therm. Eng.* **2018**, *149*, 1265−1273.
(36) Stewart, M. Alternative approach required to contain costs of remote Australian offshore gas fields *Offshore* 2013, *739*.
(37) Willyard, K. A.; Schade, G. W. Flaring in two Texas shale areas: Comparison of bottom-up with top-down volume estimates for 2012 to 2015. *Sci. Total Environ.* **2019**, *691*, 243−251.
(38) Sun, K.; Ginosar, D. M.; He, T.; Zhang, Y.; Fan, M.; Chen, R. Progress in Nonoxidative Dehydroaromatization of Methane in the Last 6 Years. *Ind. Eng. Chem. Res.* **2018**, *57*, 178−1789.
(39) Olivos-Suarez, A. I.; Szécsényi, Ag.; Hensen, E. J. M.; Ruiz-Martinez, J.; Pidko, E. A.; Gascon, J. Strategies for the Direct Catalytic Valorization of Methane Using Heterogeneous Catalysis: Challenges and Opportunities. *ACS Catal.* **2016**, *6*, 2965−2981.
(40) Kondratenko, E. V.; Peppel, T.; Seeburg, D.; Kondratenko, V. A.; Kalevaru, N.; Martin, A.; Wohlrab, S. Methane conversion into different hydrocarbons or oxygenates: current status and future perspectives in catalyst development and reactor operation. *Catal. Sci. Technol.* **2017**, *7*, 366−381.
(41) Farrell, B. L.; Igenegbai, V. O.; Linic, S. A Viewpoint on Direct Methane Conversion to Ethane and Ethylene Using Oxidative Coupling on Solid Catalysts. *ACS Catal.* **2016**, *6*, 4340−4346.
(42) Sakbodin, M.; Wu, Y.; Oh, S. C.; Wachsman, E. D.; Liu, D. Hydrogen-Permeable Tubular Membrane Reactor: Promoting Conversion and Product Selectivity for Non-Oxidative Activation of Methane over an FeVSiO2 Catalyst. *Angew. Chem. Int. Ed.* **2016**, *55*, 16149−16152.
(43) Oh, S. C.; Schulman, E.; Zhang, J.; Fan, J.; Pan, Y.; Meng, J.; Liu, D. Direct Non-Oxidative Methane Conversion in a Millisecond Catalytic Wall Reactor. *Angew. Chem. Int. Ed.* **2019**, *58*, 7083−7086.
(44) Han, S. J.; Lee, S. W.; Kim, H. W.; Kim, S. K.; Kim, Y. T. Nonoxidative Direct Conversion of Methane on Silica-Based Iron Catalysts: Effect of Catalytic Surface. *ACS Catal.* **2019**, *9*, 7984−7997.
(45) Chen, Y.; Wang, X.; Luo, X.; Lin, X.; Zhang, Y. Non-Oxidative Methane Conversion Using Lead- and Iron-Modified Albite Catalysts in Fixed-Bed Reactor. *Chin. J. Chem.* **2018**, *36*, 531−537.
(46) Okolie, C.; Lyu, Y.; Kovarik, L.; Stavitski, E.; Sievers, C. Coupling of Methane to Ethane, Ethylene, and Aromatics over Nickel on Ceria−Zirconia at Low Temperatures. *ChemCatChem* **2018**, *10*, 2700−2708.
(47) Xie, P.; Pu, T.; Nie, A.; Hwang, S.; Purdy, S. C.; Yu, W.; Su, D.; Miller, J. T.; Wang, C. Nanoceria-Supported Single-Atom Platinum Catalysts for Direct Methane Conversion. *ACS Catal.* **2018**, *8*, 4044−4048.
(48) Xiao, Y.; Varma, A. Highly Selective Nonoxidative Coupling of Methane over Pt-Bi Bimetallic Catalysts. *ACS Catal.* **2018**, *8*, 2735−2740.
(49) Nishikawa, Y.; Ogihara, H.; Yamanaka, I. Liquid-Metal Indium Catalysis for Direct Dehydrogenative Conversion of Methane to Higher Hydrocarbons. *ChemistrySelect* **2017**, *2*, 4572−4576.
(50) Kim, S. K.; Kim, H. W.; Han, S. J.; Lee, S. W.; Shin, J.; Kim, Y. T. Mechanistic and microkinetic study of non-oxidative methane coupling on a single-atom iron catalyst. *Commun. Chem.* **2020**, *3*, No. 58.

https://doi.org/10.1021/acs.iecr.1c03572
Ind. Eng. Chem. Res. XXXX, XXX, XXX−XXX

(51) Postma, R. S.; Lefferts, L. Influence of axial temperature profiles on Fe/SiO2 catalyzed nonoxidative coupling of methane. *ChemCatChem* **2021**, *13*, 1157−1160.
(52) Zhao, T.; Wang, H. Methane dehydro-aromatization over Mo/HZSM-5 catalysts in the absence of oxygen: Effect of steam-treatment on catalyst stability. *J. Nat. Gas Chem.* **2011**, *20*, 547−552.
(53) Guéret, C.; Daroux, M.; Billaud, F. Methane pyrolysis: thermodynamics. *Chem. Eng. Sci.* **1997**, *52*, 815−827.
(54) Keller, G. E.; Bhasin, M. M. Synthesis of ethylene via oxidative coupling of methane: I. Determination of active catalysts. *J. Catal.* **1982**, *73*, 9−19.
(55) Arakawa, H.; Aresta, M.; Armor, J. N.; Barteau, M. A.; Beckman, E. J.; Bell, A. T.; Bercaw, J. E.; Creutz, C.; Dinjus, E.; Dixon, D. A.; Domen, K.; DuBois, D. L.; Eckert, J.; Fujita, E.; Gibson, D. H.; Goddard, W. A.; Goodman, D. W.; Keller, J.; Kubas, G. J.; Kung, H. H.; Lyons, J. E.; Manzer, L. E.; Marks, T. J.; Morokuma, K.; Nicholas, K. M.; Periana, R.; Que, L.; Rostrup-Nielson, J.; Sachtler, W. M. H.; Schmidt, L. D.; Sen, A.; Somorjai, G. A.; Stair, P. C.; Stults, B. R.; Tumas, W. Catalysis Research of Relevance to Carbon Management: Progress, Challenges, and Opportunities. *Chem. Rev.* **2001**, *101*, 953−996.
(56) Lunsford, J. H. Catalytic conversion of methane to more useful chemicals and fuels: a challenge for the 21st century. *Catal. Today* **2000**, *63*, 165−174.
(57) Luo, L.; Tang, X.; Wang, W.; Wang, Y.; Sun, S.; Qi, F.; Huang, W. Methyl Radicals in Oxidative Coupling of Methane Directly Confirmed by Synchrotron VUV Photoionization Mass Spectroscopy. *Sci. Rep.* **2013**, *3*, No. 1625.
(58) Arndt, S.; Laugel, G.; Levchenko, S.; Horn, R.; Baerns, M.; Scheffler, M.; et al. A Critical Assessment of Li/MgO-Based Catalysts for the Oxidative Coupling of Methane. *Catal. Rev.* **2011**, *53*, 424−514.
(59) Zavyalova, U.; Holena, M.; Schlögl, R.; Baerns, M. Statistical Analysis of Past Catalytic Data on Oxidative Methane Coupling for New Insights into the Composition of High-Performance Catalysts. *ChemCatChem* **2011**, *3*, 1935−1947.
(60) Kuo, J. C. W.; Kresge, C. T.; Palermo, R. E. Evaluation of direct methane conversion to higher hydrocarbons and oxygenates. *Catal. Today* **1989**, *4*, 463−470.
(61) Wozny, G.; Arellano-Garcia, H. Oxidative Coupling of Methane: A Design of Integrated Catalytic processes. *Chem. Eng. Trans.* **2010**, *21*, 1399−1404.
(62) Zeng, Y.; Akin, F. T.; Lin, Y. S. Oxidative coupling of methane on fluorite-structuredsamarium−yttrium−bismuth oxide. *Appl. Catal., A* **2001**, *213*, 33−45.
(63) Nagaki, D. A.; Zhao, Z.; Myint, M. N. Z.; Lengyel, I.; Mamedov, A.; Gundlach, C. W.; Sankaranarayanan, K.; Falcone, D. Method for Producing Hydrocarbons by Non-Oxidative Coupling of Methane. U.S. Patent US9,902,6652018.
(64) Kosinov, N.; Uslamin, E. A.; Meng, L.; Parastaev, A.; Liu, Y.; Hensen, E. J. M. Reversible Nature of Coke Formation on Mo/ZSM-5 Methane Dehydroaromatization Catalysts. *Angew. Chem. Int. Ed.* **2019**, *58*, 7068−7072.
(65) Corredor, E. C.; Chitta, P.; Deo, M. D. Techno-economic evaluation of a process for direct conversion of methane to aromatics. *Fuel Process. Technol.* **2019**, *183*, 55−61.
(66) Do, T. N.; Kim, Y. T.; Kim, J. Technical and Economic Feasibility of Direct Methane Conversion for Hydrocarbon Production: Process Design and Techno-economic Analysis. *Comput.-Aided Chem. Eng.* **2020**, *48*, 1015−1020.
(67) Gattis, S. C.; Peterson, E. R. Process for the Conversion of Natural Gas to Hydrocarbon Liquids. Mar. 24, 2005.
(68) Obradović, A.; Thybaut, J. W.; Marin, G. B. Oxidative Coupling of Methane: Opportunities for Microkinetic Model-Assisted Process Implementations. *Chem. Eng. Technol.* **2016**, *39*, 1996−2010.
(69) Zhang, Z.-G. Process, reactor and catalyst design: Towards application of direct conversion of methane to aromatics under nonoxidative conditions. *Carbon Resour. Convers.* **2019**, *2*, 157−174.
(70) Ma, S.; Guo, X.; Zhao, L.; Scott, S.; Bao, X. Recent progress in methane dehydroaromatization: From laboratory curiosities to promising technology. *J. Energy Chem.* **2013**, *22*, 1−20.
(71) Salehi, M.-S.; Askarishahi, M.; Godini, H. R.; Görke, O.; Wozny, G. Sustainable Process Design for Oxidative Coupling of Methane (OCM): Comprehensive Reactor Engineering via Computational Fluid Dynamics (CFD) Analysis of OCM Packed-Bed Membrane Reactors. *Ind. Eng. Chem.* **2016**, *55*, 3287−3299.
(72) Stünkel, S.; Trivedi, H.; Godini, H. R.; Jašo, S.; Holst, N.; Arndt, S.; Steinbach, J.; Schomäcker, R. Oxidative Coupling of Methane: Process Design, Development and Operation in a Mini-Plant Scale. *Chem. Ing. Tech.* **2012**, *84*, 1989−1996.
(73) Holmen, A.; Olsvikb, O.; Rokstad, O. A. Pyrolysis of natural gas: chemistry and process concepts. *Fuel Process. Technol.* **1995**, *42*, 249−267.
(74) National Institute of Standards and Technology NIST Chemistry Webook, SRD 69 . https://webbook.nist.gov/.
(75) Postma, R. S.; Lefferts, L. Effect of ethane and ethylene on catalytic non oxidative coupling of methane *Reaction Chemistry & Engineering*, 2021.
(76) Foss, M. M. *Interstate Natural Gas-Quality Specifications & Interchangeability*; Center for Energy Economics, 2004.
(77) Uniongas Chemical Composition of Natural Gas. https://www.uniongas.com/about-us/about-natural-gas/chemical-composition-of-natural-gas.
(78) Douglas, J. M. *Conceptual Design Chemical Processes*; McGraw-Hill Chemical Engineering Series, 1988.
(79) Barnicki, S. D.; Fair, J. R. Separation System Synthesis: A Knowledge-Based Approch 1. Liquid Mixture Separations. *Ind. Eng. Chem. Res.* **1990**, *29*, 421−432.
(80) Barnicki, S. D.; Fair, J. R. Separation System Synthesis: A Knowledge-Based Approach. 2. Gas/Vapor Mixtures. *Ind. Eng. Chem. Res.* **1992**, *31*, 1679−1694.
(81) Aspen Technology, I., Aspen Plus, 2018.
(82) Ogihara, H.; Tajima, H.; Kurokawa, H. Pyrolysis of mixtures of methane and ethane: activation of methane with the aid of radicals generated from ethane. *React. Chem. Eng.* **2020**, *5*, 145−153.
(83) Schneider, I. A. Über die Rolle des Äthans bei der thermishen Methanzersetzung. *Z. Phys. Chem.* **1963**, *223*, 234−248.
(84) Germain, J.; Vaniscotte, C., Craquage du Methane dans un Reacteur Tubulaire. 3. Effet Iniateur de l'Ethane. *bulletin de la Socíeté Chimique de France*, **1958**.
(85) Rokstad, O. A.; Olsvik, O.; Holmen, A. Thermal Coupling of Methane. In *Natural Gas Conversion*, 1991; pp 533−539.
(86) U.S. Energy Information Administration. *Electric Power Monthly*, 2020.
(87) Hub, H. *Hub Natural Gas Spot Price (Dollars per Million Btu)*. https://www.eia.gov/dnav/ng/hist/rngwhhdm.htm.
(88) Engineering ToolBox, Fuel Gases Heating Values, 2005.
(89) Technavio Global Naphthalene Market 2019-2023, 2019.
(90) Moran, S.; Henkel, K. D. Reactor Types and Their Industrial Applications. *Ullmann's Encyclopedia of Industrial Chemistry*. **2000**, 1−49.
(91) Seo, S.-T.; Won, W.; Lee, K. S.; Jung, C.; Lee, S. Repetitive control of CATOFIN process. *Korean J. Chem. Eng.* **2007**, *24*, 921−926.
(92) Alvarado, D.; Gottschlich, D. E. *Membrane Matrimony*. https://www.mtrinc.com/wp-content/uploads/2018/08/MembraneMatrimony-HydrocarbonEngineering.pdf (accessed June 27, 2020).
(93) Edlund, D. Hydrogen Membrane Technologies and Application in Fuel Processing. In *Hydrogen and Syngas Production and Purification Technologies*, Liu, K.; Song, C.; Subramani, V., Eds.; American Institute of Chemical Engineers, 2009.
(94) Zolandz, R. R.; Fleming, G. K. Gas Permeation: Applications. In *Membrane Handbook*; Van Nostrand Reinhold, 1992; pp 78−85.
(95) (MTR)', M. T. a. R. Hydrogen Purification in Refineries. https://www.mtrinc.com/our-business/refinery-and-syngas/hydrogen-purification-in-refineries/ (accessed June 27, 2020).

https://doi.org/10.1021/acs.iecr.1c03572
Ind. Eng. Chem. Res. XXXX, XXX, XXX−XXX

(96) Baker, R. W. Membranes and Modules. In *Membrane Technology and Applications*, 3rd ed.; John Wiley & Sons, Ltd, 2012.
(97) Zhang, K.; Way, D. Palladium-copper membranes for hydrogen separation. *Sep. Purif. Technol.* **2017**, *186*, 39−44.
(98) David, E.; Kopac, J. Devlopment of palladium/ceramic membranes for hydrogen separation. *Int. J. Hydrogen Energy* **2011**, *36*, 4498−4506.
(99) Yun, S.; Oyama, T. Correlations in palladium membranes for hydrogen separation: A review. *J. Membr. Sci.* **2011**, *375*, 28−45.
(100) Khatib, S. J.; Ted Oyama, S.; de Souza, K. R.; Noronha, F. B. Review of Silica Membranes for Hydrogen Separation Prepared by Chemical Vapor Deposition. In *Membrane Science and Technology*; 2011; Chapter 2, Vol. *14*, pp 25−60.
(101) Sircar, S.; Golden, a. T. C. Pressure Swing Adsorption Technology for Hydrogen Production. In *Hydrogen and Syngas Production and Purifi cation Technologies*, Liu, K.; Song, C.; Subramani, V., Eds.; American Institute of Chemical Engineers, 2010.
(102) Ploegmakers, J.; Jelsma, A. R. T.; van der Ham, A. G. J.; Nijmeijer, K. Economic Evaluation of Membrane Potential for Ethylene/Ethane Separation in a Retrofitted Hybrid Membrane-Distillation Plant Using Unisim Design. *Ind. Eng. Chem.* **2013**, *52*, 6524−6539.
(103) Leingchan, R. *Thailand Indusrty Outlook 2019-21 Petrochemical Industry*, 2019; p 12.
(104) Collin, G.; Höke, H.; Greim, H. Naphthalene and Hydronaphthalenes. In *Ullmann's Encyclopedia of Industrial Chemistry*; Wiley-VCH Verlag GmbH & Co., 2003.
(105) Shen, Z.; He, P.; Wang, A.; Harrhy, J.; Meng, S.; Peng, H.; Song, H. Conversion of naphthalene as model compound of polyaromatics to mono-aromatic hydrocarbons under the mixed hydrogen and methane atmosphere. *Fuel* **2019**, *243*, 469−477.
(106) IEA *The Future of Hydrogen*; IEA: Paris, 2019.
(107) Milligan, D.; Milligan, J. M. Equipment Costs. http://www.matche.com/.
(108) Peters, S. M.; Timmerhaus, K. D.; West, E. R. Equipment Costs: Plant Design and Economics for Chemical Engineers. http://www.mhhe.com/engcs/chemical/peters/data/ce.html.
(109) Towler, G.; Sinnot, R. *Chemical Engineering Design: Principle, Practice and Economics of Plant and Process Design*, 2nd ed.; Elsevier, 2013; pp 307−354.
(110) Vogt, E. T. C.; Weckhuysen, B. M. Fluid catalytic cracking: recent developments on the grand old lady of zeolite catalysis. *Chem. Soc. Rev.* **2015**, *44*, 7342−7370.
(111) Marketinsightsreports Global Sulfolane Market Research Report , 2018.
(112) Venezia; Nicholson; Stevenson; Rangel; Chakravarty; Lee *Argus Benzene Annual*, 2018.
(113) Industry Federation *China CN: Market Price: Monthly Avg: Organic Chemical Material: Industrial Naphthalene 90% or Above*, 2020.
(114) S&P Global *Platts Hydrogen Assessments*; 2020.
(115) Macrotrends.net Natural Gas Prices - Historical Chart. https://www.macrotrends.net/2478/natural-gas-prices-historical-chart (accessed Oct 28, 2021).
(116) Barchart.com SGX Benzene Historical Prices. https://www.barchart.com/futures/quotes/H9G21/historical-prices?orderBy=contractExpirationDate&orderDir=asc (accessed Oct 28, 2021).

https://doi.org/10.1021/acs.iecr.1c03572
Ind. Eng. Chem. Res. XXXX, XXX, XXX−XXX